

Accepted Manuscript

A service-oriented architecture for ensemble flood forecast from numerical weather prediction

Haiyun Shi, Tiejian Li, Ronghua Liu, Ji Chen, Jiaye Li, Ang Zhang, Guangqian Wang

PII: S0022-1694(15)00406-0

DOI: <http://dx.doi.org/10.1016/j.jhydrol.2015.05.056>

Reference: HYDROL 20491

To appear in: *Journal of Hydrology*

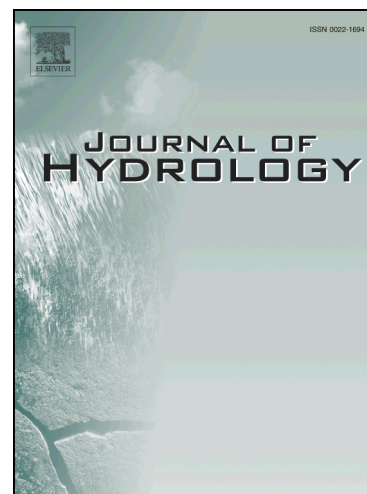
Received Date: 4 February 2015

Revised Date: 15 May 2015

Accepted Date: 28 May 2015

Please cite this article as: Shi, H., Li, T., Liu, R., Chen, J., Li, J., Zhang, A., Wang, G., A service-oriented architecture for ensemble flood forecast from numerical weather prediction, *Journal of Hydrology* (2015), doi: <http://dx.doi.org/10.1016/j.jhydrol.2015.05.056>

This is a PDF file of an unedited manuscript that has been accepted for publication. As a service to our customers we are providing this early version of the manuscript. The manuscript will undergo copyediting, typesetting, and review of the resulting proof before it is published in its final form. Please note that during the production process errors may be discovered which could affect the content, and all legal disclaimers that apply to the journal pertain.



1 **A service-oriented architecture for ensemble flood forecast from**
2 **numerical weather prediction**

3 Haiyun SHI^{a,b,*}, Tiejian LI^{a,*}, Ronghua LIU^c, Ji CHEN^b, Jiaye LI^a, Ang ZHANG^a,
4 Guangqian WANG^a

5 ^a*State Key Laboratory of Hydrosience and Engineering, Tsinghua University, Beijing, China*

6 ^b*Department of Civil Engineering, The University of Hong Kong, Pokfulam, Hong Kong, China*

7 ^c*China Institute of Water Resources and Hydropower Research, Beijing, China*

8 E-mail addresses:

9 Haiyun SHI: shihaiyun@mail.tsinghua.edu.cn

10 Tiejian LI: litiejian@tsinghua.edu.cn

11 Ronghua LIU: liurh@iwhr.com

12 Ji CHEN: jichen@hku.hk

13 Jiaye LI: thulijy@gmail.com

14 Ang ZHANG: zhanga11@mails.tsinghua.edu.cn

15 Guangqian WANG: dhhwgq@tsinghua.edu.cn

16
17 Revised manuscript for the *Journal of Hydrology*

18 May 2015

20 **SUMMARY:**

21 Floods in mountainous river basins are generally highly destructive, usually causing
22 enormous losses of lives and property. It is important and necessary to develop an effective
23 flood forecast method to prevent people from suffering flood disasters. This paper
24 proposed a general framework for a service-oriented architecture (SOA) for ensemble
25 flood forecast based on numerical weather prediction (NWP), taking advantage of state-of-
26 the-art technologies, e.g., high-accuracy NWP, high-capacity cloud computing, and an
27 interactive web service. With the predicted rainfall data derived from the NWP, which are
28 automatically downloaded, hydrological models will be driven to run on the cloud. Judging
29 from the simulation results and flood control requirements offered by users, warning
30 information about possible floods will be generated for potential sufferers and then sent to
31 them as soon as possible if needed. Moreover, by using web service in a social network,
32 users can also acquire such information on the clients and make decisions about whether to
33 prepare for possible floods. Along with the real-time updates of the NWP, simulation
34 results will be refreshed in a timely manner, and the latest warning information will always
35 be available to users. From the sample demonstrations, it is concluded that the SOA is a
36 feasible way to develop an effective ensemble flood forecast method. After being put into
37 practice, it would be valuable for preventing or reducing the losses caused by floods in
38 mountainous river basins.

39 **Keywords:** Ensemble flood forecast; Numerical weather prediction; Service-oriented
40 architecture; Cloud computing; Web service

41

42 1. Introduction

43 Mountainous regions, where the natural conditions are extremely complicated, account
44 for nearly two-thirds of the total land area in China. In such regions, high-intensity
45 rainstorms occur frequently during the flood period, which can lead to serious flood
46 disasters and cause enormous losses of lives and property to the inhabitants living in the
47 villages at the riversides or near the outlets of rivers (Caruso et al., 2013; Mazzorana et al.,
48 2013; Ruiz-Villanueva et al., 2013; Shi and Wang, 2015). According to the statistic, there
49 are 29 provinces, 274 prefecture-level cities and 1,836 county-level cities that suffer from
50 flood disasters in China, covering an area of 4.63 million km² and involving 0.56 billion
51 people. The key prevention and control area is 0.97 million km², involving 0.13 billion
52 people, among which 74 million people suffer a direct threat (Chen, 2010). Specifically,
53 the death toll caused by flash flood disasters accounted for two-thirds of the total death toll
54 caused by all flood disasters every year in China before the 1990s; the percentage has risen
55 to 80% since 2000. Approximately 4,000 people, accounting for 90% of the death toll
56 caused by all flood disasters, were dead or missing in the flash flood disasters in 2010.
57 This indicates that the situation of flood prevention and control will still be severe in the
58 future; more technical and financial support should be provided for these flood-prone
59 regions. Consequently, it is important and necessary to develop an effective flood forecast
60 method to prevent people from having to suffer flood disasters.

61 Generally, traditional methods for flood forecast include the following two types. The
62 first type comprises those methods based on critical rainfall, including the static and
63 dynamic critical rainfall methods (Carpentera et al., 1999; Georgakakos, 2006; Liu et al.,

64 2010). It is supposed that floods and some secondary disasters (e.g., debris flow and
65 landslide) may occur in a river basin when the rainfall during a certain time interval
66 reaches a certain amount or intensity (i.e., the static critical rainfall). Because the saturated
67 degree of soil or the antecedent precipitation index has an important effect on the
68 formation of floods, the critical rainfall should not be constant; thus, the dynamic critical
69 rainfall method has been developed. Overall, the critical rainfall methods are easy to use,
70 with no need for rainfall-runoff calculation; however, they cannot reflect the spatial
71 variation of rainfall, making their applications in flood forecast limited. In contrast, the
72 second type, which is applicable for river basins with sufficient, observed hydrological
73 data, comprises those methods based on critical streamflow computed by using an
74 empirical approach or hydrological models (Liu et al., 2005; Nayak et al., 2005; Cane et al.,
75 2013; Moreno et al., 2013). Comparing simulation results against the flood control
76 requirements, warnings concerning floods can be made early, if needed. Due to its high
77 forecast accuracy, this type of method has been widely used; however, limited by the
78 demand for massive observed data, it seems to be useless for river basins with poor data
79 quality, especially for ungauged river basins.

80 China has dealt with the task of flood prevention and control for a long time.
81 Moreover, more attention will be paid to floods in the future, and the construction of
82 automatic weather stations, county-level data processing centers and early warning systems
83 will be carried out in the near future. A number of provinces in China have set up their
84 own flood warning systems; however, there are still gaps between the requirements for
85 flood warning and reality. For example, a typical process of a flood warning system below
86 the county level includes several levels (e.g., county, town, village, group and family). The

87 rainfall and hydrological regime is reported to the superior level by level, and the warning
88 information is sent to the inferior level by level as well. Although such a process is in
89 accord with the status quo in China, the lengthy information transmission may
90 considerably affect the efficiency. Thus, it is important and necessary to develop a high-
91 efficiency method for flood forecast.

92 To this end, this paper aims to propose such a flood forecast method. Currently,
93 numerical weather prediction (noted as NWP hereafter), at the global scale, has developed
94 rapidly with the development of science and technology (Demeritt et al., 2007;
95 Pappenberger et al., 2008). Furthermore, service-oriented architecture (noted as SOA
96 hereafter) has been successfully applied in a wide variety of fields (Erl, 2005; Bell, 2008;
97 Linthicum, 2009); however, the application of SOA for ensemble flood forecast cannot be
98 found in the literature. As a result, this paper proposes the general framework of an SOA
99 for ensemble flood forecast based on the NWP for the first time, taking advantage of the
100 high-accuracy NWP, high-capacity cloud computing and an interactive web service. On
101 the one hand, NWP is introduced to increase the forecast lead time; on the other hand,
102 SOA is introduced to improve the forecast efficiency. In this study, the major challenges in
103 developing such a flood forecast method are i) automatically downloading and updating
104 the predicted rainfall from the NWP in real time, ii) implementing multiple scenarios for
105 flood forecast at the same time by using high performance computing (noted as HPC
106 hereafter) job scheduling, and iii) transferring warning information efficiently by using an
107 interactive web service. Due to these state-of-the-art technologies, this method would be
108 useful for preventing or reducing the losses caused by flood disasters in mountainous river
109 basins after being put into practice.

110 **2. Methodology**

111 A conceptual framework of the SOA for ensemble flood forecast based on the NWP,
112 combining the advantages of the high-accuracy NWP, high-capacity cloud computing and
113 an interactive web service, is proposed in this paper (Fig. 1). In the following, the basic
114 structures of the SOA, NWP, hydrological model used for ensemble flood forecast, HPC
115 job scheduling used for multiple scenarios, and interactive web service used for
116 information transfer will be introduced in detail.

117 *2.1. Service-oriented architecture*

118 Service-oriented architecture (SOA) is essentially a software design methodology
119 based on structured collections of discrete services that collectively provide the complete
120 functionality of a complex application (Erl, 2005). Each service is a well-defined, self-
121 contained set of functions and built as a discrete piece of code, which makes it possible to
122 reuse the code by changing only the interactions of a certain service with other ones rather
123 than the code of the service. Moreover, services communicate with each other closely,
124 involving either simple data passing or complex coordination (Bell, 2008, 2010). Hence,
125 SOA is considered as the infrastructure supporting communications between services, and
126 some connecting services are required. Currently, web service, a set of protocols enabling
127 services to be published, discovered and used in a technology neutral form, seems to be the
128 most feasible way for developing the SOA (Benslimane et al., 2008). By using a web
129 service, a service consumer (e.g., the user client) can send a request message to a service
130 provider (e.g., the cloud server), and then the service provider can return a response
131 message to the service consumer as soon as possible (Linthicum, 2009). It is worth noting

132 that the SOA is an architecture not only of services, as seen from a technology perspective,
133 but also of policies, practices and frameworks, by which we can ensure that the right
134 services are provided and consumed.

135 As shown in Fig. 1, the cloud server and user client are regarded as the two primary
136 systems in the SOA. Data collection and management, hydrological simulation, flood
137 forecast and early warning are achieved on the cloud server; meanwhile, messages of flood
138 control requirements from different users and flood early warnings from the cloud server
139 are transferred between the cloud server and user client by using a web service in a social
140 network. Fig. 2 presents the flowchart of the SOA for ensemble flood forecast based on the
141 NWP, and the details are introduced as follows.

142 First, the NWP data are downloaded automatically, in real time, from websites that
143 provide relevant data and then stored in the database on the cloud server (see Section 2.2
144 for details); moreover, flood control requirements are provided by users on the clients and
145 stored in the database as well. Second, a physically based hydrological model, the Digital
146 Yellow River Integrated Model (noted as DYRIM hereafter) (Wang et al., 2007, 2015; Li
147 et al., 2009a, 2009b), is adopted to compute the streamflow by using the NWP data; the
148 simulation results are also stored in the database. Third, judging from the comparison of
149 the simulation results against the flood control requirements from different users, flood
150 early warnings are generated, if necessary; in addition, along with the real-time updates of
151 the NWP data, the simulation results are refreshed in a timely manner so that the latest
152 early warnings are always available. Finally, by using a web service, the flood forecast and
153 early warning system on the cloud server can send warning information to the potential
154 sufferers. Moreover, users on the clients can also run the DYRIM on the cloud server by

155 themselves at any time to acquire the simulation results within the forecast lead time of the
156 NWP data so that better preparation can be made for the possible flood disasters. Overall,
157 it is clear that such a process of flood forecast and early warning is quite different from the
158 current process and is useful to the potential sufferers, affording them much more response
159 time for flood disasters.

160 *2.2. Numerical weather prediction*

161 Normally, numerical weather prediction (NWP) can be divided into two categories:
162 single NWP and ensemble NWP. The single NWP is usually insufficient for flood forecast
163 because it involves considerable uncertainties that may lead to lots of errors (Demeritt et
164 al., 2007); meanwhile, the ensemble NWP may provide an opportunity to significantly
165 improve the quality of flood forecast, including not only accuracy but also lead time
166 (Pappenberger et al., 2008). It is believable that a more accurate prediction for atmospheric
167 conditions and meteorological phenomena (e.g., rainfall) in the near future can be obtained
168 from the ensemble NWP.

169 The THORPEX (i.e., The Observing System Research and Predictability Experiment)
170 Interactive Grand Global Ensemble (noted as TIGGE hereafter) dataset is one of the
171 acknowledged NWP datasets available at present (Richardson, 2005; Park et al., 2008).
172 This dataset has been available since 2006 from ten institutions worldwide, including the
173 Bureau of Meteorology (BoM, Australia), the China Meteorological Administration
174 (CMA), the Canadian Meteorological Center (CMC), the Center for Weather Forecast and
175 Climate Studies (CPTEC, Brazil), the European Centre for Medium-Range Weather
176 Forecasts (ECMWF), the Japan Meteorological Agency (JMA), the Korea Meteorological

177 Administration (KMA), the MeteoFrance (MF), the US NCEP, and the United Kingdom
178 Meteorological Office (UKMO). All of these datasets have the same temporal resolution of
179 6 hours, while their horizontal resolutions are quite different (e.g., $9/16^\circ$ for the CMA and
180 1° for the NCEP and CMC). Moreover, the forecast lead time of the TIGGE data can be 1-
181 16 days, which indicates that the TIGGE data can be a promising tool for short- or
182 medium-term flood forecast.

183 Due to the uncertainty of the NWP, this indicates that the TIGGE datasets from
184 different institutions can provide a variety of alternatives and seem to be more suitable for
185 this study. Generally, all of these TIGGE datasets can be downloaded for free from their
186 respective official websites (e.g., <http://tigge.ecmwf.int/>). To acquire the newest rainfall
187 data in time for flood forecast, a method to automatically download and manage the NWP
188 data is proposed, taking advantage of the Htmlunit (2013) and Apache CFX web services
189 (2014). Three steps are introduced in detail as follows.

190 Step 1: Download the NWP data from the websites. In this step, operations on the
191 web browser are simulated and realized by using the Htmlunit; two tasks, including login
192 authentication and data downloading, are realized by using the source codes given in
193 Appendix A.

194 Step 2: Manage the NWP data on the cloud server. In this step, the downloaded NWP
195 data are interpreted first and then stored in a specific database. Moreover, the NWP data
196 are converted into visual images in the TIFF format (see Appendix B for the source codes).

197 Step 3: Make the above two steps autorun. In this step, the above two functions (i.e.,
198 data downloading and management) are packaged into a one by using the Apache CFX

199 web service. The program for downloading the NWP data is encapsulated as a service
200 component, which runs automatically at a fixed time interval in the background of a server;
201 moreover, this service is configured into the web server (i.e., Tomcat).

202 2.3. *Digital Yellow River Integrated Model*

203 Digital Yellow River Integrated Model (DYRIM) is a distributed model platform
204 developed by Tsinghua University for hydrological and sediment simulations in river
205 basins (Wang et al., 2007, 2015; Li et al., 2009a, 2009b). The DYRIM uses a high-
206 resolution digital drainage network that is extracted from a digital elevation model (noted
207 as DEM hereafter) (Bai et al., 2015) and coded using a modified binary tree method (Li et
208 al., 2010) to simulate runoff yield and flow routing on each hillslope-channel unit.
209 Moreover, dynamic parallel computing technology based on sub-basin decomposition has
210 been developed to speed up the simulation (Li et al., 2011; Wang et al., 2011, 2012; Wu et
211 al., 2013).

212 The DYRIM hydrological model is a physically based distributed model that
213 represents the infiltration-excess runoff yield mechanism. This model uses a hillslope-
214 channel as a basic hydrological unit because of the different hydrological response
215 mechanisms of hillslopes and channels. The runoff-yield model is established based on the
216 hillslope unit, where the soil mass is divided into topsoil and subsoil layers. A variety of
217 hydrological processes are simulated, including vegetation interception, evapotranspiration,
218 infiltration-excess runoff on the surface, subsurface flow in these two layers, and water
219 exchange between these two layers. In the DYRIM hydrological model, the temporal
220 resolution is six minutes and the rainfall data are uniformly assigned to each time step;

221 moreover, the rainfall data are spatially interpolated by using the inverse distance weighted
222 method. It is worth noting that parameters in the DYRIM hydrological model can be
223 divided into two types: (i) invariant parameters used for describing the properties of land
224 use and soil type, influenced by the basic features of the river basin and determined from
225 the literature, fieldwork and prior studies; and (ii) adjustable parameters that are calibrated
226 and verified with the observed data.

227 *2.4. HPC job scheduling*

228 HPC is an important branch of computer science that focuses on the development of
229 high performance computers and relevant software. It is a technology that can improve the
230 capability of scientific computing through organizing a number of processors or computers
231 as members of a cluster; it is based on parallel computing technology, a way of enabling an
232 application to be divided into multiple parts that can be executed in parallel multiple
233 processors. There are several types of HPC systems (e.g., large clusters and highly
234 specialized hardware), most of which are based on clusters and interconnect with each
235 other by using a high performance network, e.g., the Quad Data Rate (QDR) InfiniBand
236 network. HPC allows scientists and engineers to solve complex scientific, engineering and
237 business problems by using applications that require high bandwidth, low latency
238 networking, and very high computing capability. In the future, HPC will be more
239 networked, open, standard, structured and diversified in application. For example, in the
240 field of hydrological simulation, HPC can be used when a parallel hydrological model (e.g.,
241 the DYRIM in this study) is applied in large-scale river basins.

242 The framework of the SOA for ensemble flood forecast based on the NWP in this
243 study tries to provide a two-layer parallelism (Fig. 3). The lower layer is the parallelism in
244 the DYRIM hydrological model; the upper layer is the parallelism in the hydrological
245 simulations with the NWP data from different institutions, which is realized by using a job
246 scheduling function. Moreover, the Windows HPC Server 2012 used in this study has 24
247 compute nodes with 20 processor cores on each of them, i.e., 480 processor cores in total.
248 Generally, one processor core can execute only one process each time; using more
249 processor cores at one time means less time consumption. The number of processor cores
250 used for hydrological simulation at one time can significantly affect the efficiency of the
251 lower-layer parallelism and further affect the efficiency of the upper-layer parallelism.
252 Namely, if N processor cores are used for hydrological simulation with the NWP data from
253 one institution, then hydrological simulations with the NWP data from $\text{INT}(480/N)$ (note:
254 the symbolic function $\text{INT}(X)$ means the integer part of a real number X) institutions can be
255 carried out at the same time by using the HPC job scheduling.

256 2.5. Web service

257 An interactive web service is developed to receive the flood control requirements
258 from the users and send early warnings to the users. Moreover, it is also used for queries
259 on a variety of hydrological information (e.g., the digital drainage network, historical and
260 predicted rainfall data, and streamflow predictions). All of the data are stored in the
261 databases on the cloud server and can be inquired by the user clients at any time. For
262 example, based on the global drainage network (Bai et al., 2015) extracted from the 30-m-
263 resolution Advanced Spaceborne Thermal Emission and Reflection Radiometer (ASTER)

264 Global DEM dataset (ASTER GDEM Validation Team, 2009, 2011), users can define a
265 watershed by specifying the location of the watershed outlet (i.e., longitude and latitude)
266 and the corresponding river reach. Then, the drainage network of the entire watershed will
267 be selected for hydrological simulation (i.e., flood forecast).

268 **3. Results and discussions**

269 In this study, two river basins in China, including the Juma River basin in the
270 southwest suburb of Beijing and the upper Baishui River basin in the north of Sichuan
271 province, are regarded as the study areas for the application of the SOA for ensemble flood
272 forecast based on the NWP. In the following, the available research data used for each case
273 are introduced, and the results as well as discussions are presented.

274 *3.1. Case study of the Juma River basin*

275 The Juma River basin is located in the southwest of Beijing ($114^{\circ}27'-115^{\circ}47'$ E,
276 $39^{\circ}12'-40^{\circ}04'$ N). As shown in Fig. 4, there is only one hydrological station (i.e., the
277 Zhangfang hydrological station) in this river basin; the drainage area in the upstream of
278 this station is over $3,800 \text{ km}^2$. The high-resolution digital drainage network is also shown
279 in Fig. 4; there are 25,833 river reaches and nearly 65,000 hillslopes in total in the
280 extracted digital drainage network.

281 The Juma River basin was severely affected by the notorious rainstorm on July 21,
282 2012, in Beijing. This rainstorm was characterized by a large rainfall depth, long duration
283 and high intensity. According to the information from the Beijing Water Authority, this
284 rainstorm lasted for nearly 16 hours, and the mean rainfall depth of the whole city was 170

285 mm, with a significantly uneven spatial distribution. For example, the Fangshan District, in
286 the southwest of Beijing, had the maximum rainfall depth of 301 mm, while Yanqing
287 County, in the northwest, had the minimum rainfall depth of 69 mm. The area with a
288 rainfall depth over 200 mm was approximately 6,000 km², covering 36% of the total area
289 of Beijing, and the largest point rainfall (i.e., 460 mm, with a return period of 500 years)
290 occurred in the Fangshan District. As a result, approximately 1.9 million people had
291 property loss, and among them, 0.8 million were in the Fangshan District; furthermore,
292 there were 79 persons killed due to this rainstorm.

293 To accurately forecast floods due to severe rainfall, the reliable estimation of rainfall
294 is paramount; then, hydrological models can be used to forecast streamflow with more
295 accuracy. In this case, the TIGGE data derived from six of the above-mentioned ten
296 institutions (i.e., the CMA, CMC, CPTEC, ECMWF, NCEP and UKMO) are selected as
297 the research data (i.e., the predicted rainfall data) because there was no data available from
298 the other four institutions for the period of this rainstorm. After being downloaded
299 automatically in real time from the official websites (see Section 2.2 for details), the NWP
300 data are used as the basic input data for the follow-up streamflow simulation and flood
301 forecast. The NWP data (i.e., the TIGGE data in this study) are considered to be an
302 important factor that can affect the result of streamflow simulation; thus, it is possible that
303 using the NWP data derived from different sources may lead to different flood forecast
304 results.

305 To investigate the features of the various NWP data, the spatial distributions of total
306 rainfall depth in Beijing and the surrounding area during the time period of 0:00-24:00
307 UTC, July 21, 2012, which were described by the TIGGE data derived from six institutions

308 (i.e., the CMA, CMC, CPTEC, ECMWF, NCEP and UKMO) released at 0:00 UTC, July
309 21, 2012, were shown in Fig. 5. Overall, the six TIGGE datasets have significantly
310 different features for describing the spatial distribution of rainfall depth. On the one hand,
311 the maximum values of total rainfall depth inside the Juma River basin during this period
312 varied widely, e.g., 58.5 mm for the CMA data, 68.9 mm for the CMC data, 61.2 mm for
313 the CPTEC data, 92.5 mm for the ECMWF data, 134.8 mm for the NCEP data and 151.9
314 mm for the UKMO data; the highest value was nearly three times as much as the lowest
315 one. On the other hand, the rainfall centers described by these six TIGGE datasets during
316 this period appeared in different locations. For example, the rainfall center described by the
317 ECMWF data appeared in the downstream of the Juma River basin (Fig. 5d) but that
318 described by the UKMO data appeared in the upstream of this river basin (Fig. 5f);
319 moreover, for the NCEP data, heavy rainfall almost covered the entire river basin (Fig. 5e).

320 Furthermore, to evaluate the performances of the various NWP data in flood forecast,
321 streamflow processes of the reach where the Zhangfang hydrological station is located
322 were computed with these six TIGGE datasets by using the DYRIM hydrological model
323 and HPC job scheduling. Because the features of these six TIGGE datasets for describing
324 the spatial distribution of rainfall depth were significantly different, it is presumable that
325 the simulation results would be different (see Fig. 6). In this study, the parameters derived
326 from the previous study (Shi, 2013) were directly used, and Fig. 6 shows the comparisons
327 of streamflows computed with the six TIGGE datasets against the observed data recorded
328 at the Zhangfang hydrological station. Overall, all of the simulated values computed with
329 these six TIGGE datasets were not close to the observed ones. Only by using the NCEP
330 data or UKMO data could the peak flow be simulated; however, both the peak value and

331 appearance time were not accurate when they were compared with those presented by the
332 observed data (approximately 2,500 m³/s appeared at 23:00 UTC, July 21, 2012). By using
333 the NCEP data, the computed peak value was approximately 3,800 m³/s, 52% larger than
334 the observed peak value, and the appearance time was six hours in advance; by using the
335 UKMO data, the computed peak value was approximately 2,600 m³/s, only 4% larger than
336 the observed peak value, and the appearance time was only four hours in advance. It is
337 inferred that the UKMO data showed much better performance than the NCEP data for this
338 case. In addition, no peak flows could be simulated by using the other four TIGGE datasets
339 (i.e., the CMA, CMC, CPTEC and ECMWF).

340 Furthermore, Table 1 lists the results of streamflow simulation by using these six
341 TIGGE datasets. It is observed that the simulation results were markedly different as a
342 whole. The values of flood volume were $3.92 \times 10^6 \text{ m}^3$ (-95.27%) for the CMA data,
343 $3.98 \times 10^6 \text{ m}^3$ (-95.20%) for the CMC data, $3.94 \times 10^6 \text{ m}^3$ (-95.26%) for the CPTEC data, and
344 $3.92 \times 10^6 \text{ m}^3$ (-95.27%) for the ECMWF data. For these four TIGGE datasets, the intensity
345 of the predicted rainfall was not high enough for the runoff yield; the computed streamflow
346 was actually the base flow, resulting in no peak flows appearing. If so, no floods would
347 occur in the Juma River basin, which indicated that people living in this river basin would
348 be safe. In contrast, the high intensity of the predicted rainfall for the other two datasets led
349 to extremely large values of flood volume, e.g., $156.76 \times 10^6 \text{ m}^3$ (88.98%) for the NCEP
350 data and $112.17 \times 10^6 \text{ m}^3$ (35.23%) for the UKMO data; moreover, as mentioned above, the
351 peak values were very large as well (i.e., 3,800 m³/s for the NCEP data and 2,600 m³/s for
352 the UKMO data); enormous losses of lives and property would be caused by such large
353 floods if they came true.

354 3.2. Case study of the upper Baishui River basin

355 The upper Baishui River basin is located in the north of Sichuan province (103°22'-
356 103°47' E, 33°06'-33°40' N). The region in the upstream of the Batun hydrological station
357 with an area of 1,198 km² is considered in this study (Fig. 7). The four rainfall stations
358 with hourly observed data are also shown in Fig. 7. Moreover, there are 7,019 river reaches
359 and nearly 17,500 hillslopes in total in the extracted digital drainage network.

360 For this river basin, the flood occurred during July 16-23, 2010 is regarded as the
361 study case. The TIGGE data derived from four of the above-mentioned ten institutions (i.e.,
362 the CMA, CPTEC, ECMWF and UKMO) are selected as the research data (i.e., the
363 predicted rainfall data), as the data from the other six institutions are not available during
364 this period. Fig. 8 shows the comparison of the simulated streamflows calibrated with the
365 observed station rainfall against the observed streamflows recorded at the Batun station,
366 and the results were generally satisfactory when they were compared with those presented
367 by the observed data (approximately 75 m³/s appeared at 3:00 UTC, July 17, 2010), with
368 peak value error of -17% and peak time error of six hours delay (Table 2). Fig. 8 also
369 shows the comparisons of streamflows computed with the four TIGGE datasets against the
370 observed data recorded at the Batun station. Overall, the results computed with these four
371 TIGGE datasets were not so close to the observed data. Only by using the ECMWF data or
372 CMA data could the peak flow be simulated; however, both the peak value and appearance
373 time were not accurate. Table 2 also lists the comparisons of streamflows computed with
374 the observed station rainfall and the four TIGGE predicted rainfall inputs against the
375 observed data recorded at the Batun station. Using the predicted rainfall, the simulated
376 peak value and time were 36.0 m³/s (-52%) and six hours later for the ECMWF data and

377 30.4 m³/s (-56%) and 7 hours later for the CMA data; no peak flow could be forecasted by
378 using the CPTEC and UKMO data.

379 3.3. Discussions

380 From the case studies, it can be seen that the results of flood forecast obtained by
381 using different NWP data can be markedly different, even completely opposite. To this end,
382 it is important and necessary to provide these various results of streamflow computation by
383 using different NWP data for users at the same time. In this study, implementing multiple
384 scenarios of flood forecast (i.e., streamflow simulations by using different NWP data) at
385 the same time can be realized by using the two-layer paralleled HPC job scheduling on the
386 cloud server (see Section 2.4 for details). Generally, these simulations can be completed
387 within a few minutes (e.g., 3 minutes for the first case and 2 minutes for the second case).
388 Thereafter, all of the simulation results will be compared with the flood control
389 requirements offered by users, and the probability of flood can be described by the
390 percentage of possible floods that are simulated with different NWP data (i.e., 2 in 6 for
391 the first case and 2 in 4 for the second case). If needed, relevant warning information of
392 floods will be generated and sent to potential sufferers immediately. In addition, users on
393 the clients can also acquire such warning information by using the web service in a social
394 network at any time.

395 Generally, methods for flood risk and vulnerability analyses have been proposed for
396 ensemble flood forecast (UNDRO, 1991; Willows and Connell, 2003; Wu et al., 2012).
397 For river basins with sufficient historical hydrological data, the frequency of the predicted
398 peak flow from each NWP data can be obtained from the probability distribution function

399 derived from the observed streamflow series. Meanwhile, the critical frequency of flood to
400 cause potential disaster can be determined for each NWP agency. Thereafter, through
401 comparing the forecasted frequency of peak flow from each NWP agency against its
402 critical frequency, flood risk degree can be evaluated separately. Finally, a method to
403 generate a synthetic warning from the separate risks, considering different weights
404 according to the historical performance of each NWP agency, is needed. This method is
405 hoped to be adopted in the proposed system in future work. However, for river basins with
406 no historical hydrological data, this method is still tough to succeed. Therefore, the
407 proposed system can only provide the various flood forecast results for users at this stage.
408 After being put into practice for years, accumulation of hydrological data may make a
409 result interpretation method more applicable to the proposed system, which is much more
410 useful to provide the decision-support for users.

411 Furthermore, it can be inferred that the discrepancies in peak values and times are
412 mainly caused by the low temporal-spatial resolution of the predicted rainfall data. For
413 flood forecast in any given river basin, the globally available predicted rainfall from the
414 NWP (e.g., TIGGE) data is not accurate enough. Nevertheless, the proposed system has
415 made the techniques and the platform ready for better flood forecast, when better predicted
416 rainfall data can be obtained from much finer national and regional NWP data.

417 **4. Conclusions**

418 This paper proposed a conceptual framework for the SOA for ensemble flood forecast
419 from the NWP, combining the advantages of state-of-the-art technologies, e.g., high-
420 accuracy NWP, high-capacity cloud computing and an interactive web service. The

421 significance of this paper can be concluded as follows: first, a method to automatically
422 download and update the predicted rainfall derived from the NWP (e.g., the TIGGE data)
423 in real time was developed. Second, HPC job scheduling was adopted to implement
424 multiple scenarios of flood forecast at the same time; accordingly, various results of
425 streamflow simulation could be provided, and the latest warning information of floods
426 could be generated for potential sufferers. Third, by using the interactive web service in a
427 social network, users can either acquire such warning information on the clients at any
428 time or be informed to prepare for possible floods. It is concluded that the SOA will be a
429 feasible way for ensemble flood forecast based on the NWP, affording potential sufferers
430 much more response time when confronted with possible floods. After being put into
431 practice, the proposed system would be useful for preventing or reducing the losses caused
432 by flood disasters in mountainous river basins.

433

434 **Acknowledgements**

435 This study was supported by the National Science & Technology Pillar Program in the
436 Twelfth Five-year Plan Period (Grant No. 2013BAB05B03, 2013BAB05B05), the China
437 Postdoctoral Science Foundation funded project (Grant No. 2014M550069) and the Hong
438 Kong Scholars Program project (Grant No. XJ2014059). We are also grateful to the two
439 anonymous reviewers who offered insightful comments leading to the improvement of this
440 paper.

441

ACCEPTED MANUSCRIPT

442 **Appendix A**

443 Source codes for downloading the NWP data from websites are given as follows:

444 Login authentication:

```
445 WebClient client = new WebClient(BrowserVersion.FIREFOX_10);  
446 HtmlPage homePage = client.getPage("URL");  
447 HtmlInput name = homePage.getInputByName("Name");  
448 name.setValueAttribute("Value");  
449 HtmlPage loginPage = homePage.getAnchorByText("Name of Link").click();
```

450

451 Data downloading:

```
452 URL url = new URL(downloadurl);  
453 URLConnection conn = url.openConnection();  
454 InputStream inStream = conn.getInputStream();  
455 filestream = new FileOutputStream("@Path"+filename+".grib");  
456 datewriter.write(filename);  
457 datewriter.flush();  
458 byte[] buffer = new byte[1204];  
459 while ((byteread = inStream.read(buffer)) != -1){  
460     bytesum += byteread;  
461     filestream.write(buffer, 0, byteread);  
462 }
```

463

464 **Appendix B**

465 Source codes for the NWP data interpretation are given as follows:

466 Data interpretation:

```
467 public class GridData; //the class of rainfall data
468 String filepath = "F:\data.grib";
469 File fileptr = new File(filepath);
470 FileInputStream filestream = new FileInputStream(fileptr);
471 BufferedInputStream bufferstream = new BufferedInputStream(filestream);
472 private void GridSection(BufferedInputStream bufferstream, List<GridData> Points);
473 private void ProductSection(BufferedInputStream bufferstream);
474 private void DataSection(BufferedInputStream bufferstream, List<Double> PointsValue) throws
475 IOException {
476     int Length = ConvertInt(4, bufferstream, "the total length");
477     ConvertInt(1, bufferstream, "the serial number");
478     bufferstream.mark(Integer.MAX_VALUE);
479     for (int i = 0; i < TotalNumberofPoints; i++) {
480         double PValue = ConvertPoint(24, bufferstream, "第" + (i + 1) + "点 : ");
481         PointsValue.add(PValue);
482     }
483     bufferstream.reset();
484     bufferstream.skip(Length - 5);
485 }
```

486

487

488 **References**

- 489 Apache CFX, 2014. <<http://cxf.apache.org/>>.
- 490 ASTER GDEM Validation Team. 2009. ASTER global DEM validation summary report.
491 METI & NASA.
- 492 ASTER GDEM Validation Team. 2011. ASTER global DEM version 2 – summary of
493 validation results. METI & NASA.
- 494 Bai, R., Li, T.J., Huang, Y.F., Li, J.Y., Wang, G.Q., 2015. An efficient and comprehensive
495 method for drainage network extraction from DEM with billions of pixels using a
496 size-balanced binary search tree. *Geomorphology*, DOI:
497 10.1016/j.geomorph.2015.02.028.
- 498 Bell, M., 2008. *Service-Oriented Modeling: Service Analysis, Design, and Architecture*.
499 Wiley, New Jersey.
- 500 Bell, M., 2010. *SOA Modeling Patterns for Service Oriented Discovery and Analysis*.
501 Wiley, New Jersey.
- 502 Benslimane, D., Dustdar, S., Sheth, A., 2008. Services Mashups: The New Generation of
503 Web Applications. *IEEE Internet Computing*, 10(5), 13-15.
- 504 Cane, D., Ghigo, S., Rabuffetti, D., Milelli, M., 2013. Real-time flood forecasting coupling
505 different postprocessing techniques of precipitation forecast ensembles with a
506 distributed hydrological model. The case study of May 2008 flood in western
507 Piemonte, Italy. *Natural Hazards and Earth System Sciences*, 13(2), 211-220.

- 508 Carpentera, T.M., Sperflage, J.A., Georgakakos, K.P., Sweeney, T., Fread, D.L., 1999.
509 National threshold runoff estimation utilizing GIS in support of operational flash
510 flood warning systems. *Journal of Hydrology*, 224, 21-44.
- 511 Caruso, B.S., Rademaker, M., Balme, A., Cochrane, T.A., 2013. Flood modelling in a high
512 country mountain catchment, New Zealand: comparing statistical and deterministic
513 model estimates for ecological flows. *Hydrological Sciences Journal*, 58(2), 328-
514 341.
- 515 Chen, L., 2010. The speech in the start video conference of the construction of the non-
516 engineering measures in the mountain flood prevention at the county level. Beijing.
517 [In Chinese]
- 518 Demeritt, D., Cloke, H., Pappenberger, F., Thielen, J., Bartholmes, J., Ramos, M.-H., 2007.
519 Ensemble predictions and perceptions of risk, uncertainty, and error in flood
520 forecasting. *Environmental Hazards*, 7(2), 115-127.
- 521 Erl, T., 2005. *Service-Oriented Architecture: Concepts, Technology, and Design*. Prentice
522 Hall, New Jersey.
- 523 Georgakakos, K.P., 2006. Analytical results for operational flash flood guidance. *Journal*
524 *of Hydrology*, 317, 81-103.
- 525 HtmlUnit, 2013. <<http://htmlunit.sourceforge.net/>>.
- 526 Li, T.J., Wang, G.Q., Chen, J., 2010. A modified binary tree codification of drainage
527 networks to support complex hydrological models. *Computers & Geosciences*,
528 36(11), 1427-1435.
- 529 Li, T.J., Wang, G.Q., Chen, J., Wang, H., 2011. Dynamic parallelization of hydrological
530 model simulations. *Environmental Modelling & Software*, 26, 1736-1746.

- 531 Li, T.J., Wang, G.Q., Huang, Y.F., Fu, X.D., 2009a. Modeling the Process of Hillslope
532 Soil Erosion in the Loess Plateau. *Journal of Environmental Informatics*, 14(1), 1-
533 10.
- 534 Li, T.J., Wang, G.Q., Xue, H., Wang, K., 2009b. Soil erosion and sediment transport in the
535 gullied Loess Plateau: Scale effects and their mechanisms. *Science in China Series*
536 *E - Technological Sciences*, 52(5), 1283-1292.
- 537 Linthicum, D.S., 2009. *Cloud Computing and SOA Convergence in Your Enterprise: A*
538 *Step-by-Step Guide*. Pearson Education, New Jersey.
- 539 Liu, Z.Y., Martina, M.L., Todini, E., 2005. Flood forecasting using a fully distributed
540 model: application of the TOPKAPI model to the Upper Xixian Catchment.
541 *Hydrology and Earth System Sciences*, 9(4), 347-364.
- 542 Liu, Z.Y., Yang, D.W., Hu, J.W., 2010. Dynamic critical rainfall-based torrential flood
543 early warning for medium-small rivers. *Journal of Beijing Normal University*,
544 46(3), 317-318. [In Chinese]
- 545 Mazzorana, B., Comiti, F., Fuchs, S., 2013. A structured approach to enhance flood hazard
546 assessment in mountain streams. *Natural Hazards*, 67(3), 991-1009.
- 547 Moreno, H.A., Vivoni, E.R., Gochis, D.J., 2013. Limits to flood forecasting in the
548 Colorado Front Range for two summer convection periods using radar nowcasting
549 and a distributed hydrologic model. *Journal of Hydrometeorology*, 14(4): 1075-
550 1097.
- 551 Nayak, P.C., Sudheer, K.P., Ramasastri, K.S., 2005. Fuzzy computing based rainfall-runoff
552 model for real time flood forecasting. *Hydrological Processes*, 19(4), 955-968.

- 553 Pappenberger, F., Bartholmes, J., Thielen, J., Cloke, H.L., Buizza, R., Roo, A., 2008. New
554 dimensions in early flood warning across the globe using grand-ensemble weather
555 predictions. *Geophysical Research Letters*, 35(10), L10404.
- 556 Park, Y.-Y., Buizza, R., Leutbecher, M., 2008. TIGGE: Preliminary results on comparing
557 and combining ensembles. *European Centre for Medium-Range Weather Forecasts*,
558 Reading.
- 559 Richardson, D., 2005. The THORPEX Interactive Grand Global Ensemble (TIGGE).
560 *Geophysical Research Abstracts*, 7, Abstract EGU05-A-02815.
- 561 Ruiz-Villanueva, V., Bodoque, J.M., Diez-Herrero, A., Eguibar, M.A., Pardo-Iguzquiza, E.,
562 2013. Reconstruction of a flash flood with large wood transport and its influence on
563 hazard patterns in an ungauged mountain basin. *Hydrological Processes*, 27(24),
564 3424-3437.
- 565 Shi, H.Y., 2013. Computation of spatially distributed rainfall by merging raingauge
566 measurements, satellite observations and topographic information: A case study of
567 the 21 July 2012 rainstorm in Beijing, China. *The 35th IAHR World Congress*,
568 Chengdu, China.
- 569 Shi, H.Y., Wang, G.Q., 2015. Impacts of climate change and hydraulic structures on runoff
570 and sediment discharge in the middle Yellow River. *Hydrological Processes*, DOI:
571 10.1002/hyp.10439.
- 572 United Nations Disaster Relief Organization (UNDRO), 1991. *Mitigating Natural*
573 *Disasters: Phenomena, Effects and Options: A Manual for Policy makers and*
574 *Planners*. New York: United Nations, 1-164.

- 575 Wang, G.Q., Fu, X.D., Shi, H.Y., Li, T.J., 2015. Watershed Sediment Dynamics and
576 Modeling: A Watershed Modeling System for Yellow River. In Yang C.T. and
577 Wang L.K. (eds), *Advances in Water Resources Engineering, Handbook of*
578 *Environmental Engineering, Volume 14*. Springer International Publishing.
- 579 Wang, G.Q., Wu, B.S., Li, T.J., 2007. Digital Yellow River model. *Journal of Hydro-*
580 *Environment Research*, 1, 1-11.
- 581 Wang, H., Fu, X.D., Wang, G.Q., Li, T.J., Gao, J., 2011. A common parallel computing
582 framework for modeling hydrological processes of river basins. *Parallel Computing*,
583 37, 302-315.
- 584 Wang, H., Zhou, Y., Fu, X.D., Gao, J., Wang, G.Q., 2012. Maximum speedup ratio curve
585 (MSC) in parallel computing of the binary-tree-based drainage network. *Computers*
586 *& Geosciences*, 38, 127-135.
- 587 Willows, R.I., Connell, R.K., 2003. Climate adaptation: Risk, uncertainty and decision-
588 making. *United Kingdom: UK Climate Impacts Programme*, 39(9): 829-840.
- 589 Wu, H., Adler, R.F., Hong, Y., Tian, Y.D., Policelli, F., 2012. Evaluation of Global Flood
590 Detection Using Satellite-Based Rainfall and a Hydrologic Model. *Journal of*
591 *Hydrometeorology*, 13, 1268-1284.
- 592 Wu, Y.P., Li, T.J., Sun, L.Q., Chen, J., 2013. Parallelization of a hydrological model using
593 the message passing interface. *Environmental Modelling & Software*, 43, 124-132.
- 594

595

596

List of figure captions

597 **Fig. 1.** The framework of the service-oriented architecture (SOA) for ensemble flood forecast from
598 numerical weather prediction (NWP).

599 **Fig. 2.** The flowchart of the SOA for ensemble flood forecast from the NWP.

600 **Fig. 3.** The HPC job scheduling used in this study.

601 **Fig. 4.** The location and the digital drainage network of the Juma River basin.

602 **Fig. 5.** The spatial distributions of rainfall depth in Beijing and the surrounding area during 0:00-
603 24:00 UTC, July 21, 2012, which were described by six TIGGE datasets (i.e., the CMA,
604 CMC, CPTEC, ECMWF, NCEP and UKMO) released at 0:00 UTC, July 21, 2012.

605 **Fig. 6.** Comparison of the streamflows computed with the six TIGGE datasets against the observed
606 streamflow data recorded at the Zhangfang hydrological station.

607 **Fig. 7.** The location and the digital drainage network of the upper Baishui River basin.

608 **Fig. 8.** Comparison of the streamflows computed with the observed station rainfall and the four
609 TIGGE datasets against the observed streamflow data recorded at the Batun hydrological
610 station.

611

612

Figure 1

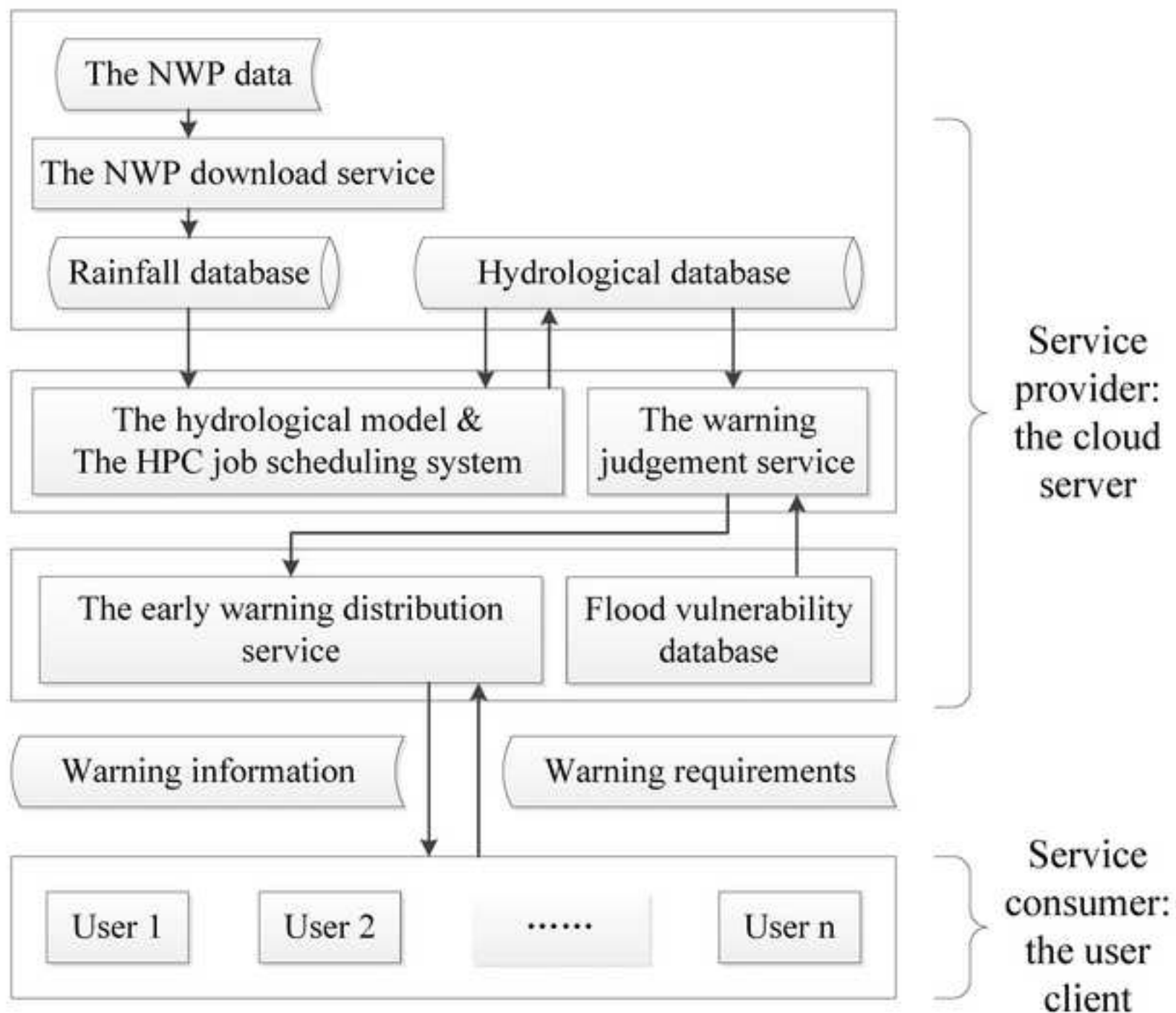
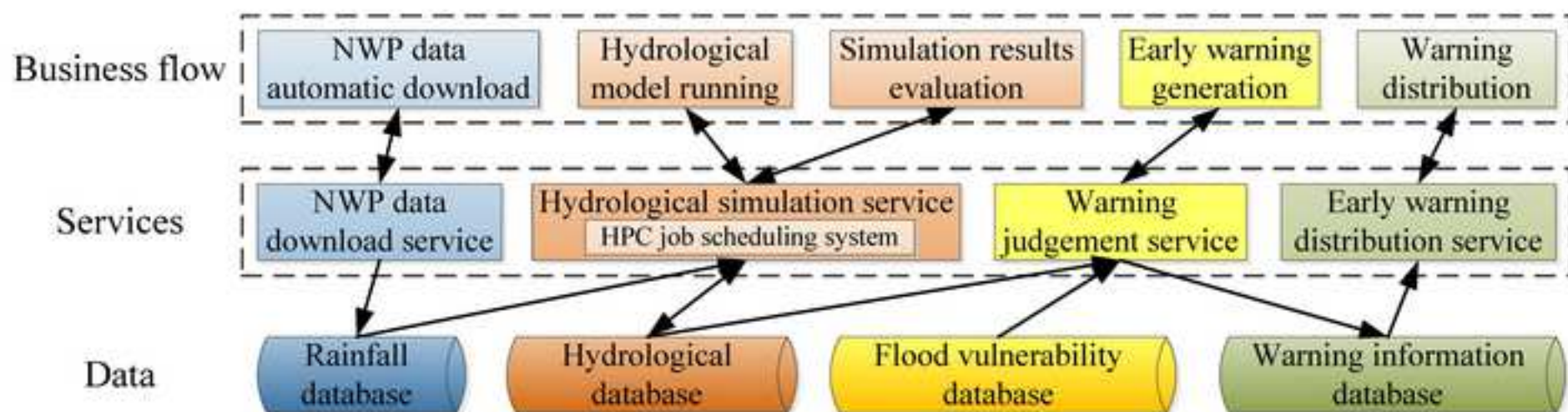


Figure 2



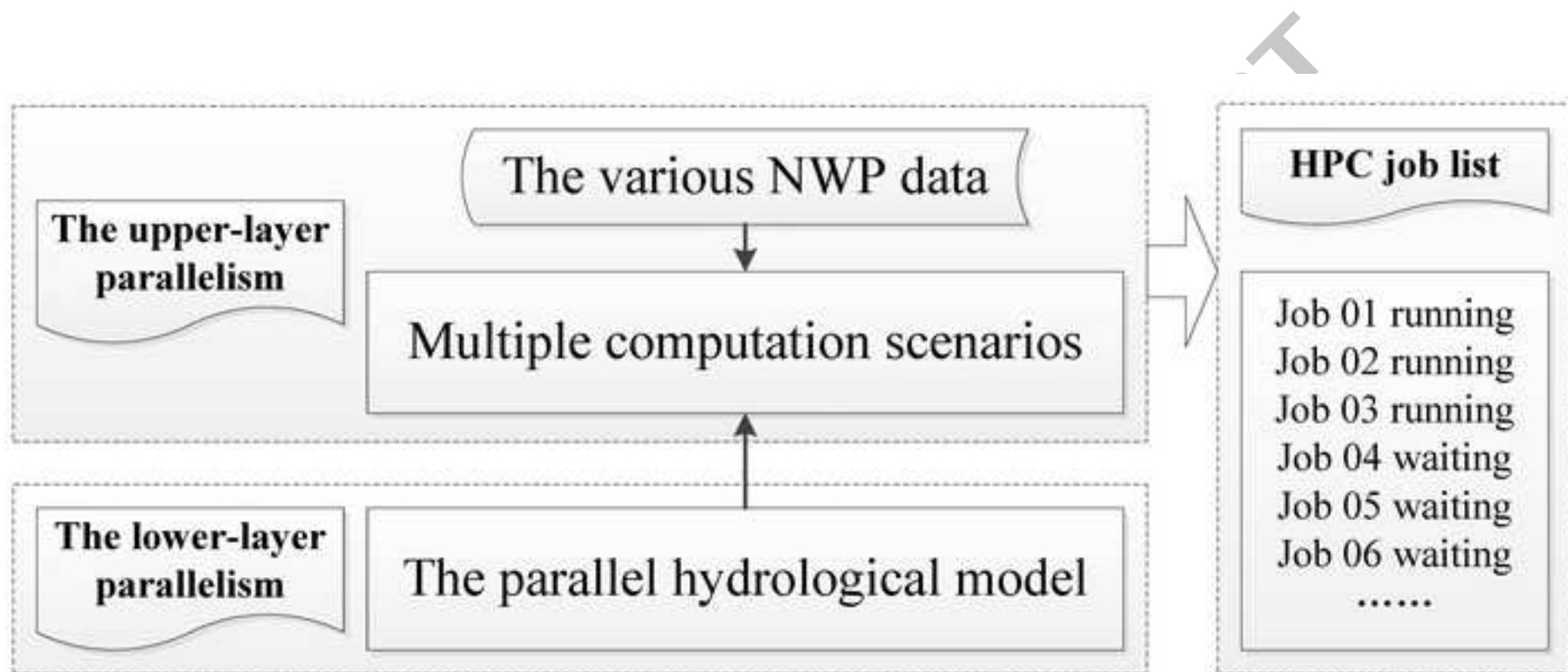
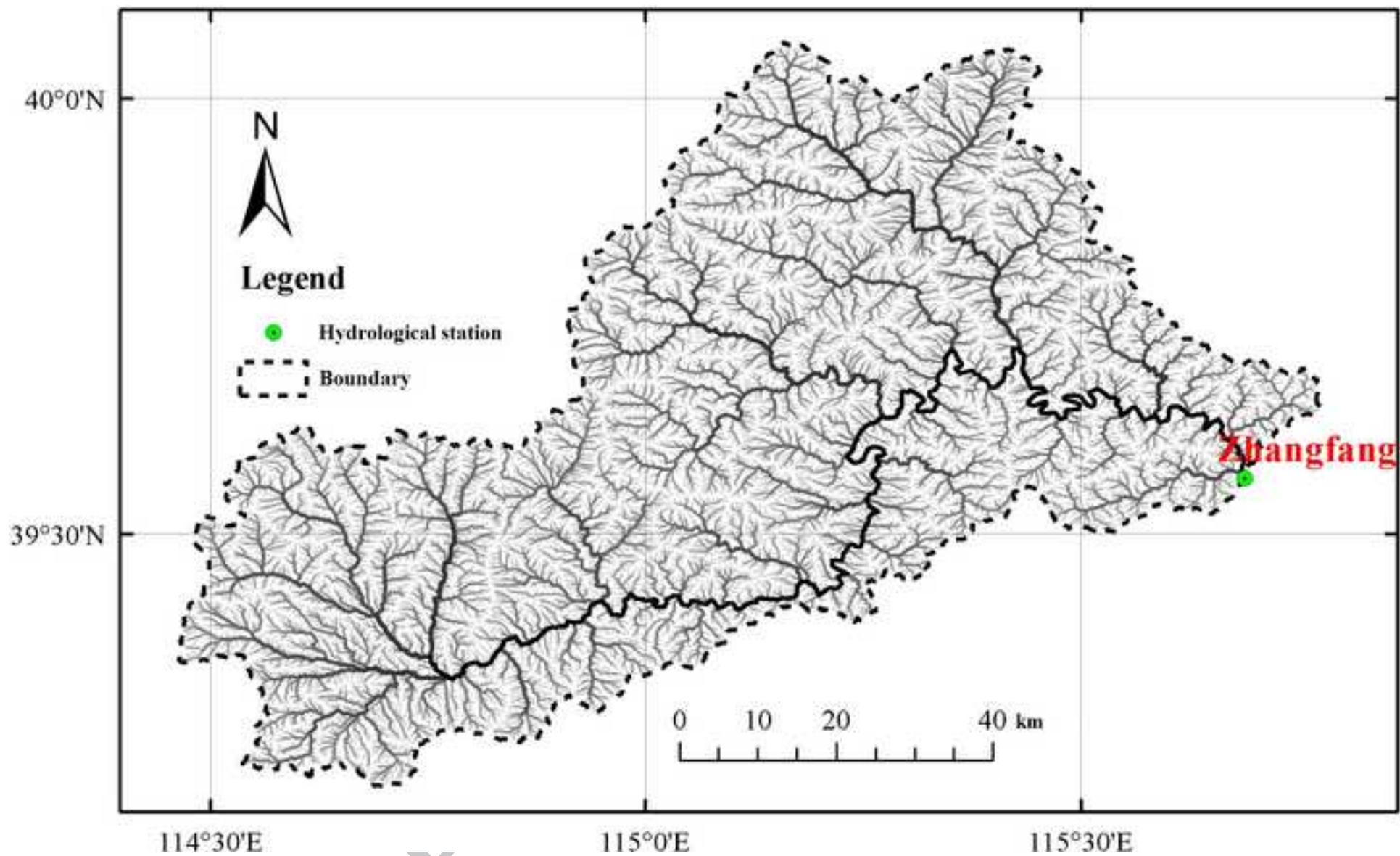


Figure 4



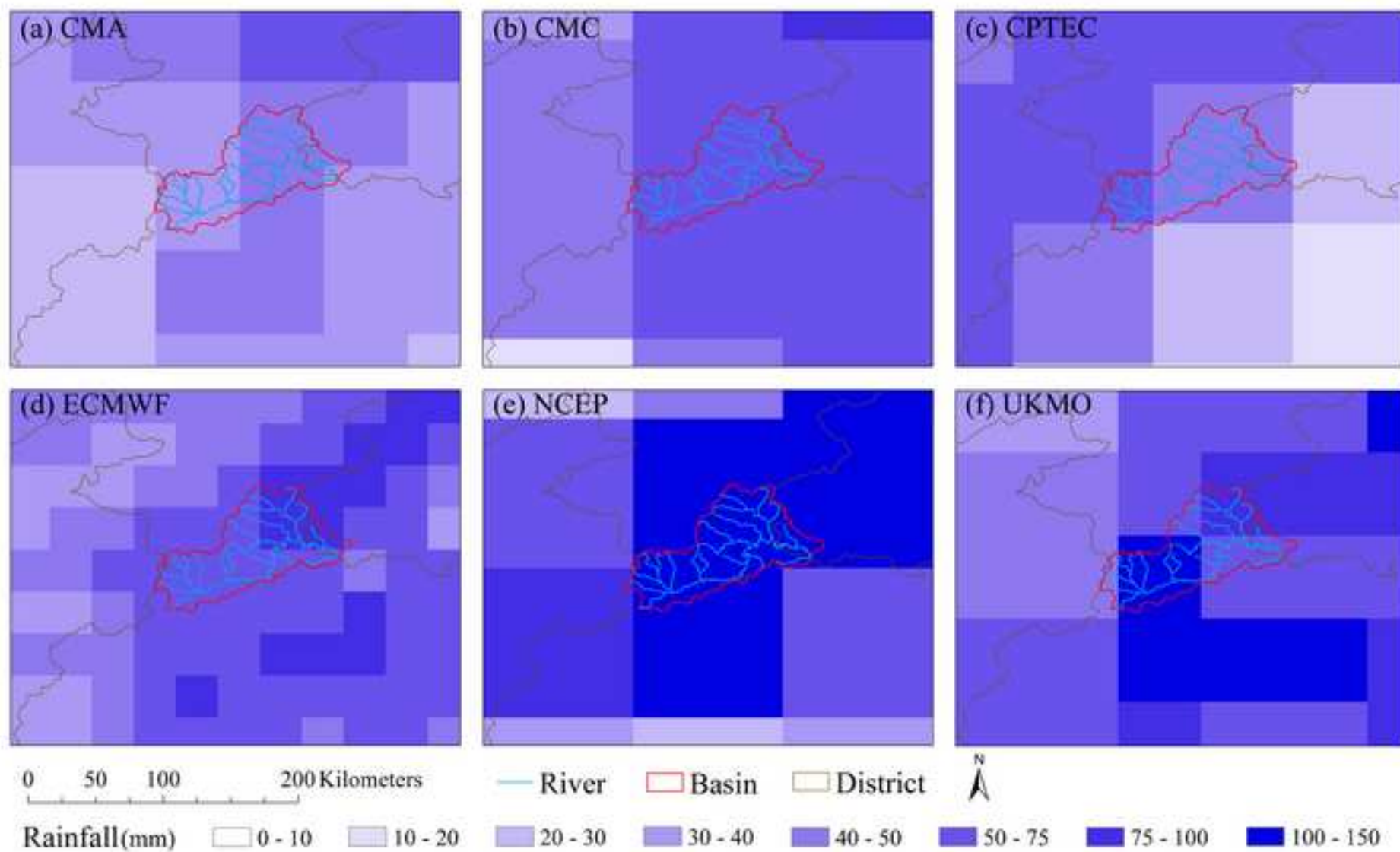
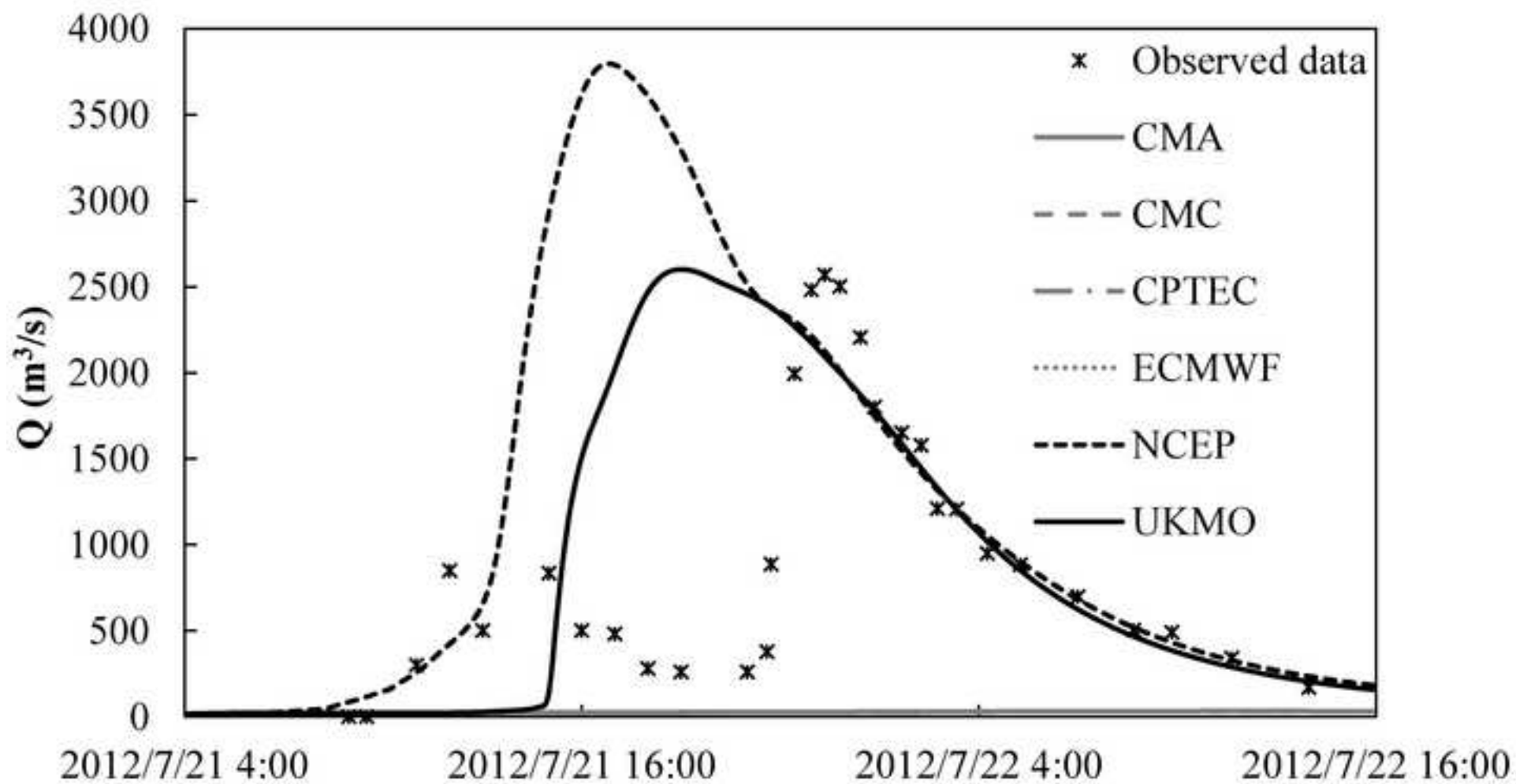


Figure 6



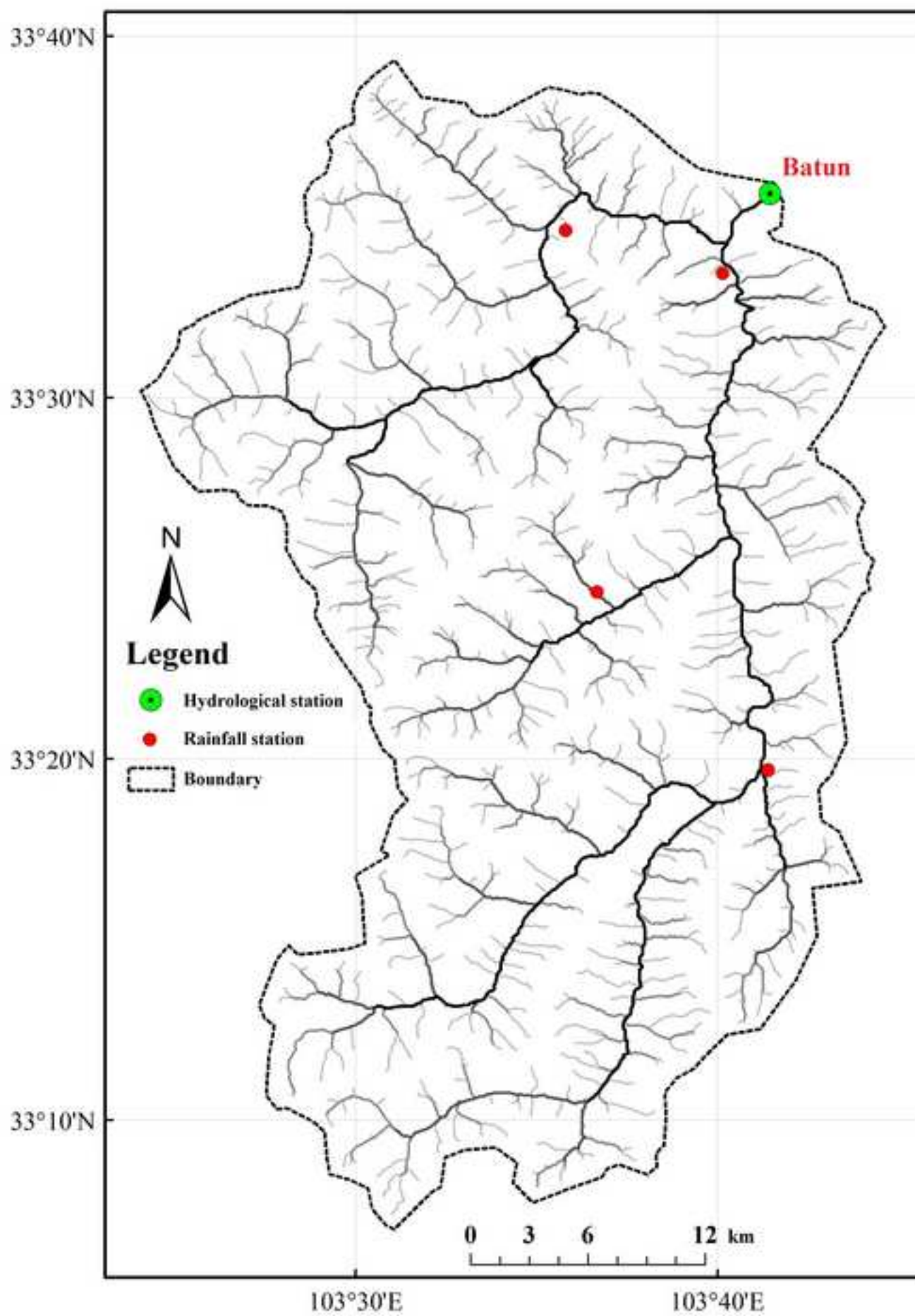
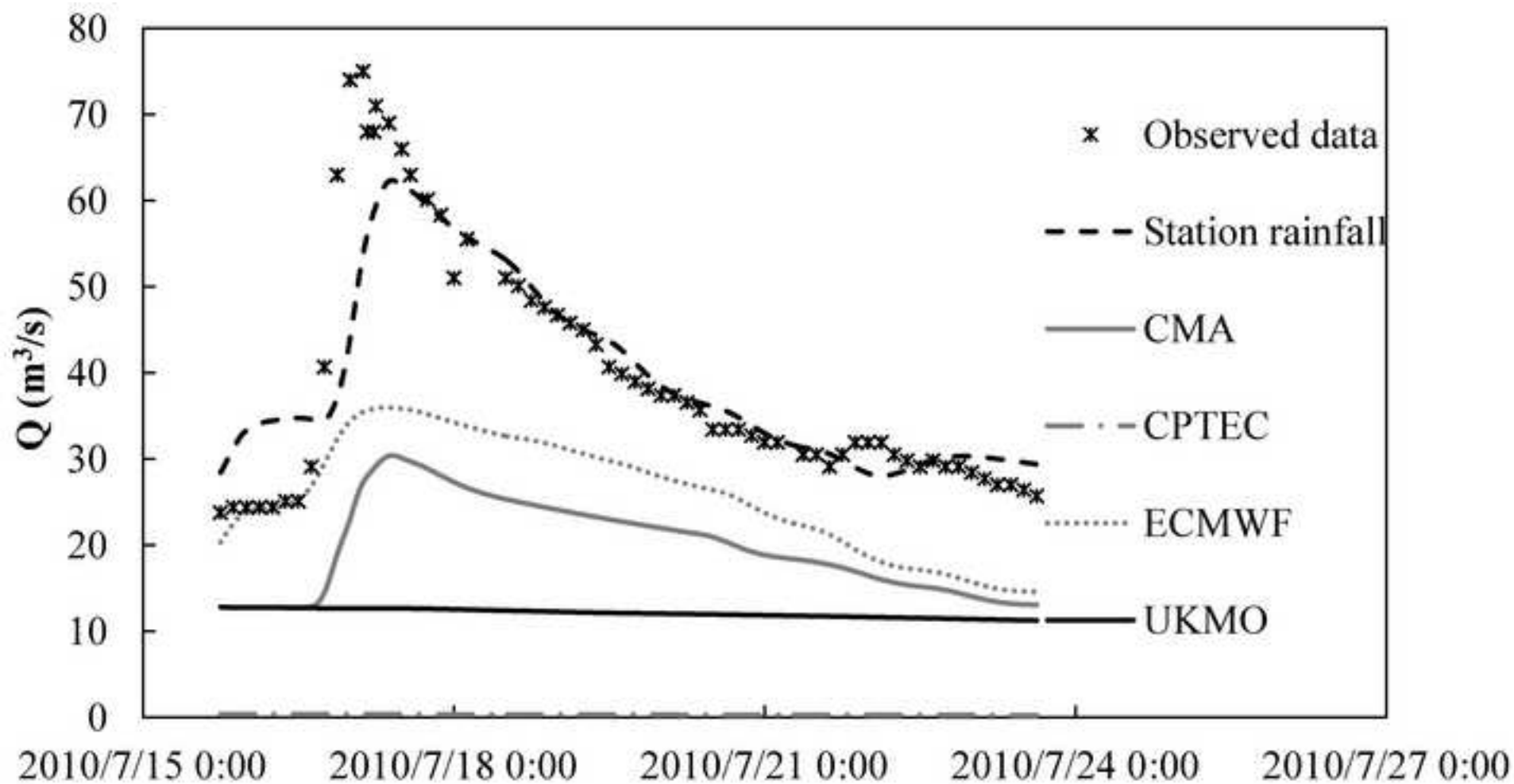


Figure 8



613

614 Table 1 Results of streamflow computation by using six different TIGGE data in the Juma River

615 basin.

Data	Flood volume (10^6 m^3)	Relative error (%)	Peak value (m^3/s)	Relative error (%)	Peak time (UTC)	Peak time error
Observation	82.95	/	2,500	/	2012/7/21 23:00	/
CMA	3.92	-95.27	/	/	/	/
CMC	3.98	-95.20	/	/	/	/
CPTEC	3.94	-95.26	/	/	/	/
ECMWF	3.92	-95.27	/	/	/	/
NCEP	156.76	+88.98	3,800	+52	2012/7/21 17:00	-6 hours
UKMO	112.17	+35.23	2,600	+4	2012/7/21 19:00	-4 hours

616

617

618

619 Table 2 Results of streamflow computation by using six different TIGGE data in the upper Baishui

620 River basin.

Data	Flood volume (10^6 m^3)	Relative error (%)	Peak value (m^3/s)	Relative error (%)	Peak time (UTC)	Peak time error
Observation	26.94	/	75.0	/	2010/7/17 3:00	/
Station rainfall (Calibration)	26.92	-0.06	62.3	-17	2010/7/17 9:00	+6 hours
CMA	13.55	-49.72	30.4	-56	2010/7/17 10:00	+7 hours
CPTEC	0.22	-99.17	/	/	/	/
ECMWF	17.68	-34.35	36.0	-52	2010/7/17 9:00	+6 hours
UKMO	8.25	-69.36	/	/	/	/

621

622

623

624

Research Highlights

- 625 1. Development of the framework of SOA for ensemble flood forecast from NWP
- 626 2. Development of a method to automatically download and update the NWP
- 627 3. Realization of implementing multiple scenarios of flood forecast at the same time
- 628 4. Validation of the new method through simulating flood flow at two river basins

629

630

ACCEPTED MANUSCRIPT